

# Multiscale Computation of Fluid and Ion Transport in Nanochannels: The Effect of Partial Charges

Sony Joseph, Aveek N. Chatterjee and N. R. Aluru \*

Department of Mechanical Engineering &  
Beckman Institute of Advanced Science and Technology,  
University of Illinois at Urbana Champaign, IL-61801, USA

\*Email: aluru@uiuc.edu

## ABSTRACT

Effects of nanoscale confinement and partial charges that stem from quantum calculations are investigated by using a hierarchical multiscale methodology in silica slit channels filled with 1 M KCl. Partial charges of both bulk and surface atoms from abinitio quantum calculations that take into account bond polarization is used in molecular dynamics simulations to obtain ion and water concentration profiles for channel widths of 1.371, 2.235 and 3.09 nm. By simulating corresponding channels with no partial charges it was observed that the partial charges affect the concentration profiles till a distance of about 0.8 nm from the surface. Both in the uncharged and charged cases, oscillations in concentration profiles of  $K^+$  and  $Cl^-$  ions gives rise to an electroosmotic flow in the presence of an external electric field contrary to the expectations from continuum theory. The I-V characteristics are significantly altered by partial charges for slits less than 2.5 nm in width.

**Keywords:** nanofluidics, silica channels, partial charges, electroosmotic flow.

## 1 INTRODUCTION

Transport and electrochemical phenomena in synthetic nanochannels is of growing interest in biomimetic nanoscale devices. Recent advances in the fabrication of “lab on a chip” ultra-confined fluidic systems [1][2] and synthetic nanopores [3] raise fundamental questions about the influence of surfaces on ion transport. The surface charges induce electrostatic ion (Debye) screening and electrokinetic effects such as electro-osmosis can have large effects on conductance in nanochannels. Electrolyte-oxide interfaces play a key role in detection, precipitation or adsorption of toxic agents. The silica-electrolyte interfacial dynamics and the effects of nanoscale confinement on the transport properties of ions and water need to be resolved for characterization and design of silica nanochannel based devices and sensors.

Traditionally Poisson-Boltzman (PB) or Poisson Nernst Planck (PNP) equations are used in continuum theory to calculate the ionic concentration profile away from a surface. Such models for the calculation of the electrostatic interaction energies assume a smooth smeared out surface

charge. In real systems the charges are discrete. Finite size of the ions and ion-ion correlations are also neglected. Finally continuum theories neglect the structure of water along with water-surface and water-water interactions.

Though atomic scale simulations can be used to explicitly treat the finite size of ions and water, it is possible that in nanoscale channels the contribution of the quantum effects on the electrostatic interactions of the wall, such as the bond polarization effects can influence fluid transport properties. However, the extremely small order of time and length scales possible in abinitio density functional theory (DFT) and atomistic molecular dynamics (MD) simulations make them unsuitable for a full-scale device characterization. We employed a hierarchical multiscale approach that takes into account the quantum effects, by first calculating the atomic partial charges using the DFT, and then using these as inputs for the MD simulations to calculate the transport coefficients and finally using these values in the PNP equations to calculate the current-voltage characteristics.

We investigated electrolytic transport in  $\alpha$ -quartz channels of three different widths (3.09 nm, 2.235 nm and 1.371 nm) with 1 M KCl. The computational domain consisting of the surface atoms and confined electrolyte is shown in Figure 1. The surface chemistry of silica-water interface is quite complex [9] and depends on the type of surface - hydroxylated or dehydroxylated. In this paper we consider a neutral dehydroxylated surface. Both partially charged and uncharged cases were studied.

## 2 COMPUTATION OF QUANTUM PARTIAL CHARGES

Even though the surface may not have any net charge, localized electron density distribution due to the difference in electron affinity of silicon and oxygen and the effects of bond polarization, can be represented by partial charges on the atoms. Quantum calculations were performed both for the surface and bulk silica using Gaussian 03 to obtain the charge density. We used a periodic density functional approach with exchange correlation using the B3LYP formulation and a 6-31G\* split valence polarization basis set. For the bulk, a single unit cell with 6 Si and 3 O atoms

were used with periodic boundary condition in all three directions. Table 1 compares our results with some commonly used force fields in literature.

| Force field         | Teppen <i>et al</i> [5] | van Duin <i>et al</i> [6] | Present calculation |
|---------------------|-------------------------|---------------------------|---------------------|
| $q_{Si}$ bulk       | 1.4                     | 1.346                     | 1.3                 |
| $q_O$ bulk          | -0.7                    | -0.673                    | -0.65               |
| System type         | OH terminated cluster   | OH terminated Cluster     | Periodic            |
| Quantum calculation | MP2                     | DFT                       | DFT                 |
| Partial charge      | Chelpg                  | Mulliken                  | Mulliken            |

Table 1: Comparison of our bulk partial charges with that in literature.

For computing surface partial charges a structure comprising of  $1 \times 1 \times 3$  unit cells was used with one end terminated with OH groups as shown in Figure 1. Periodic boundaries were used in  $x$  and  $y$  directions. The resulting partial charges are also shown. The partial charges computed are the Mulliken partial charges. For non periodic clusters, by fitting point charges to the molecular electrostatic potential, Chelpg partial charges can be computed. For large non periodic clusters we observed that the difference between Mulliken and Chelpg partial charges are not significant.

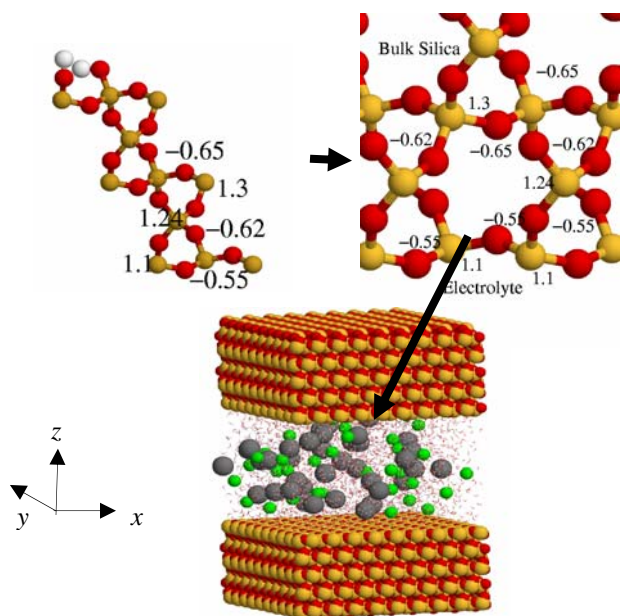


Figure 1: Partial charge computations for the wall atoms in the silicon dioxide membrane. On the bottom is the MD simulation domain and on the top are the partial charges from silica surface DFT calculations.

### 3 MOLECULAR DYNAMICS SIMULATIONS

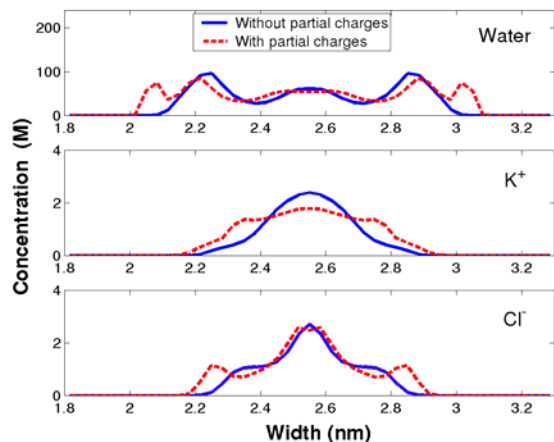
Molecular dynamics simulations were performed with computed partial charges using modified GROMACS [7]. Figure 1 shows the schematic of the system. The wall is made of 101  $\alpha$ -quartz surface which is symmetric with respect to the channel axis. The channel wall thickness is 2 nm. The wall silicon and oxygen atoms were fixed in space. The LJ parameters for ion-ion and ion-water pairs were taken from [8], and those for the ion-Si and O-Si pairs were obtained by using the linear combination rule and the Si-Si parameters from [7]. The ions are modeled as Lennard Jones atoms with point charges. The silica slab on both sides had dimensions of  $4.5 \times 5.4 \times 2$  nm<sup>3</sup> and the channel widths were 1.371, 2.235 and 3.09 nm. The SPC/E model was used for water with constraints using the SHAKE algorithm. Periodic boundary conditions were used in the  $x$  and  $y$  directions. Berendsen thermostat was used to maintain the temperature at 300 K. Electrostatic interactions were computed using a 2D periodic PME [9].

#### 3.1 Water structure

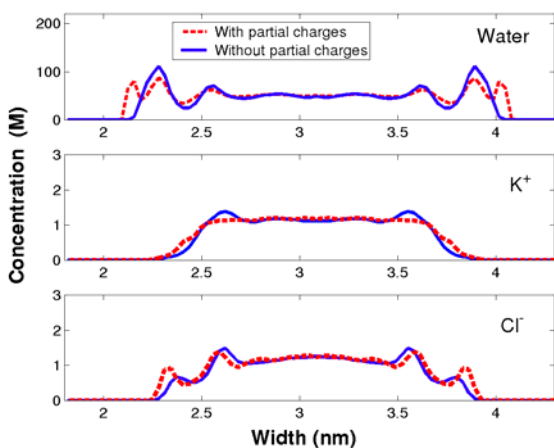
Molecular dynamics simulations with these partial charges show significant variation in the water ordering and structure in the nanochannel with and without partial charges. Concentration variations were observed both in the axial and transverse directions. Without partial charges one observes the well known layering effects. As shown in Figure 2, with partial charges water is pulled closer to the wall with the formation of a peak of adsorbed water and this effect is more pronounced at smaller slit widths. Such an adsorption has also been observed in other water-oxide interfaces in experiments [10]. Partial charges also seem to suppress the layering of the water near the wall, reducing the peak heights and decreasing the depths of the valleys. The effect of the partial charges on the water concentration profiles seems to be significant till a distance of 0.8 nm from the surface.

As channel width decreases, the layering starts to overlap and there is no bulk-like region. Both confinement and partial charges influence the fluid layering. For uncharged 1.371 nm slits the water dipole is mainly oriented at an angle of  $90^\circ$  to the normal to the surface of the channel because of the confinement. Partial charges enhance the ordering of water. When the channel is charged, the water in the adsorbed region is oriented at an angle of  $60^\circ$ - $70^\circ$  to the normal in such a way that they form hydrogen bonds with the wall surface and non adsorbed water near the surface is oriented so as to form hydrogen bonds towards the water away from the surface. Vibrational spectroscopy experiments [11] show that at crystalline  $\alpha$ -quartz water interfaces, the ordering is enhanced causing the formation of ice like structures in the adsorbed layer with a more ordered hydrogen bonding network.

a) 1.371 nm



b) 2.235 nm



c) 3.09 nm

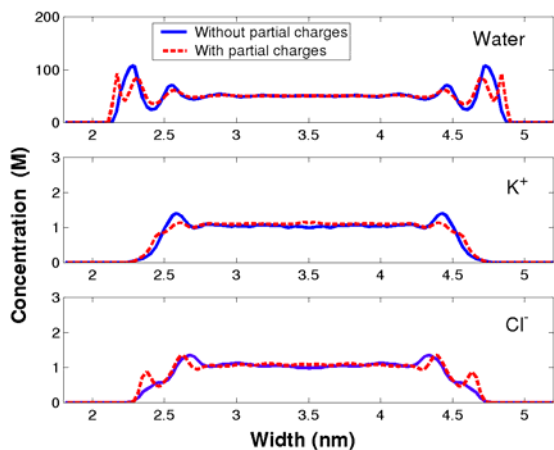


Figure 2: Comparison of concentration profiles of water,  $K^+$ ,  $Cl^-$  ions with and without partial charges. The closest wall atom to the water is at 2 nm distance in the figure above.

### 3.2 Ion concentration profiles

Contrary to the classical continuum theory expectations, when there are no partial charges, there are oscillations in the ion concentration profiles due to the finite size effects of the ions and  $Cl^-$  ions are found to be closer to the wall than  $K^+$  ions with a small peak near the wall (Figure 3). For charged surfaces, Qiao and Aluru [12] have observed similar peaks for  $Na^+$  and  $Cl^-$  ions and they have explained the peaks citing different interactions of the co and counter ions with water. Criss-crossing of counter and co-ions are more pronounced and the ions are pulled closer to the wall when the slits have partial charges.

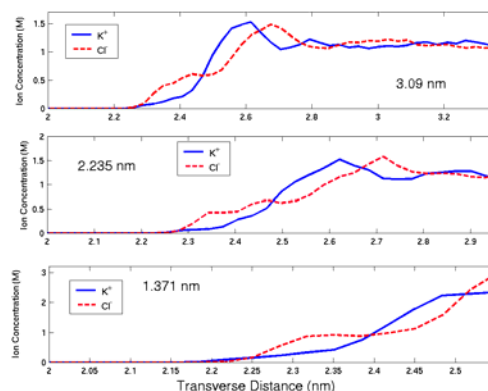


Figure 3: Comparison of  $K^+$  and  $Cl^-$  ion concentration profile for the uncharged slits of three different widths with and without partial charges.

Figure 4 shows that the location of the peaks in concentration occurs when the potential of the mean force is at a minimum. Near the surface,  $Cl^-$  has slightly more negative PMF than  $K^+$  and so is preferred over  $K^+$ .

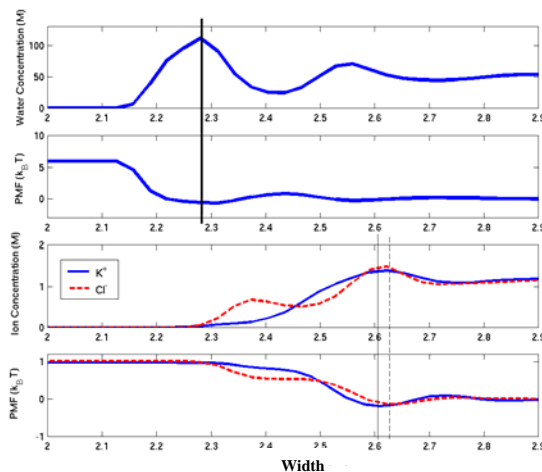


Figure 4: Water and ion concentrations for the 2.235 nm channel and the corresponding potential of mean force.

### 3.3 Electroosmotic flow

In the presence of an external electric field of 0.5 V/nm, these oscillations in ion concentration profiles give rise to electroosmotic flow even though the solution in the channel is electroneutral (Figure 5). Electroosmotic flow is also observed in slits with partial charges. However, it is smaller because of the stronger electrostatic interactions of water with the surface, which increases the viscosity near the surface. When the co-ion and counter ion concentrations are the same, no electroosmotic flow is expected in continuum theory because it is unable to capture the concentration variation due to the layering effects.

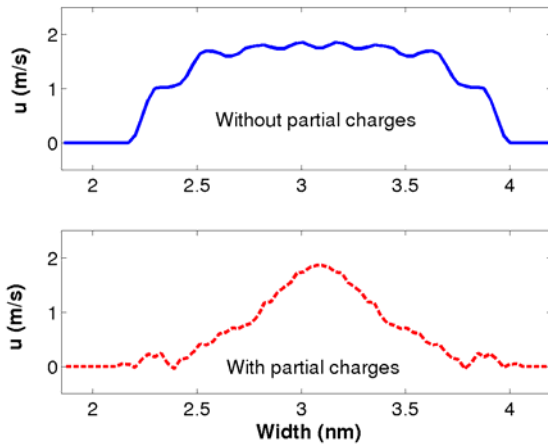


Figure 5: Electroosmotic flow in a 2.235 nm channel with and without partial charges.

### 4 CONTINUUM CALCULATIONS

The diffusion coefficients are computed from molecular dynamics simulations by calculating the slope of the mean square displacement of the ions (Table 2). As expected, the diffusion coefficients are smaller for charged cases. These coefficients are used to calculate the mobility of the ions to be used in continuum theory. I-V characteristics from the continuum theory (Figure 6), shows that for widths greater than 3 nm, the effect of the partial charges on the IV curve is minimal. However, for the channels with widths of the order of 1-2 nm, the effect of the partial charges on the I-V characteristics is substantial.

| $D \times 10^{-9} \text{ m}^2/\text{s}$ | Without partial charges |               | With partial charges |               |
|---|-------------------------|---------------|----------------------|---------------|
|   | $\text{K}^+$            | $\text{Cl}^-$ | $\text{K}^+$         | $\text{Cl}^-$ |
| 1.371 nm                                | 1.40                    | 1.20          | 0.71                 | 0.62          |
| 2.235 nm                                | 1.50                    | 1.38          | 1.20                 | 0.99          |
| 3.09 nm                                 | 1.66                    | 1.50          | 1.66                 | 1.46          |

Table 2: Diffusion coefficients for different widths.

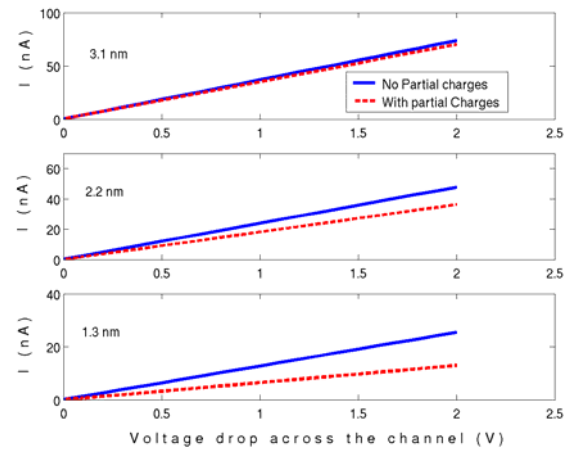


Figure 6 I-V profiles, with and without partial charges, in large (3.09 nm), medium (2.235 nm) and small (1.371 nm) channels.

### 5 CONCLUSIONS

In summary, we demonstrate a hierarchical multiscale methodology to solve ion transport in nanoscale channels and show that the partial charges from quantum calculations significantly alter transport properties and I-V plots for electrolytes in confined geometries. The quantum contributions of the wall–electrolyte interactions are substantial in channel widths of the order of 1-2 nm. Electroosmotic flow is observed in charged and uncharged channels because of the oscillations in ion density, which creates a local net charge density.

### Acknowledgements

This work was supported by the National Science Foundation through the Nano-CEMMS center under grant No. 0328162.

### REFERENCES

- [1] H. Cao *et al.*, *Appl. Phys. Lett.* **81**, 174 (2002).
- [2] J. Li *et al.*, *Nature* (London) **412**, 166 (2001).
- [3] J. Storm *et al.*, *Nature Mater.* **2**, 537 (2003).
- [4] R. K. Iler and R. K. Aler, *The Chemistry of Silica* (Wiley, New York, 1978), 1st ed.
- [5] B. J. Teppen *et al.*, *Phys. Chem. B*, **101** (9), 1579 (1997).
- [6] C. T. van Duin, *et al.*, *J. Phys. Chem. A* **107**, 3803 (2003).
- [7] E. Lindahl, *et al.*, *J. Mol. Model.* **7**, 306 (2001).
- [8] D. E. Smith and L. X. Dang, *J. Chem. Phys.* **100**, 3757 (1994).
- [9] I. Yeh and M. Berkowitz, *J. Chem. Phys.* **111**, 3155 (1999).
- [10] Q. Du *et al.*, *Phys. Rev. Lett.* **72** (2), 238 (1994).
- [11] V. Ostroverkhov *et al.*, *Chemical Physics Letters*, **386** (1-3), 144 (2003).
- [12] R. Qiao and N. R. Aluru, *J. Chem. Phys.* **118** (10), 4692 (2003).